



Article

The Combined Inactivation of Intestinal and Hepatic ZIP14 Exacerbates Manganese Overload in Mice

Caitlin K. Fung and Ningning Zhao *

School of Nutritional Sciences and Wellness, The University of Arizona, Tucson, AZ 85721, USA;
caitlinfung@email.arizona.edu

* Correspondence: zhaonn@email.arizona.edu; Tel.: +520-621-9744

Abstract: ZIP14 is a newly identified manganese transporter with high levels of expression in the small intestine and the liver. Loss-of-function mutations in *ZIP14* can lead to systemic manganese overload, which primarily affects the central nervous system, causing neurological disorders. To elucidate the roles of intestinal ZIP14 and hepatic ZIP14 in maintaining systemic manganese homeostasis, we generated mice with single-tissue or two-tissue *Zip14* knockout, including intestine-specific (*Zip14*-In-KO), liver-specific (*Zip14*-L-KO), and double (intestine and liver) *Zip14*-knockout (*Zip14*-DKO) mice. *Zip14*^{flox/flox} mice were used as the control. Tissue manganese contents in these mice were compared using inductively coupled plasma mass spectrometry (ICP-MS) analysis. We discovered that although the deletion of intestinal ZIP14 only moderately increased systemic manganese loading, the deletion of both intestinal and hepatic ZIP14 greatly exacerbated the body's manganese burden. Our results provide new knowledge to further the understanding of manganese metabolism, and offer important insights into the mechanisms underlying systemic manganese overload caused by the loss of ZIP14.

Keywords: ZIP14; *SLC39A14*; manganese; intestine; liver; nutrition



Citation: Fung, C.K.; Zhao, N. The Combined Inactivation of Intestinal and Hepatic ZIP14 Exacerbates Manganese Overload in Mice. *Int. J. Mol. Sci.* **2022**, *23*, 6495. <https://doi.org/10.3390/ijms23126495>

Academic Editor: Dariusz Chlubek

Received: 26 April 2022

Accepted: 9 June 2022

Published: 10 June 2022

Publisher's Note: MDPI stays neutral with regard to jurisdictional claims in published maps and institutional affiliations.



Copyright: © 2022 by the authors. Licensee MDPI, Basel, Switzerland. This article is an open access article distributed under the terms and conditions of the Creative Commons Attribution (CC BY) license (<https://creativecommons.org/licenses/by/4.0/>).

1. Introduction

Manganese is an essential nutrient. Manganese deficiency leads to impaired growth, osteoporosis, dyslipidemia, asthma, and cognitive defects. Excess manganese in the body is toxic, and produces a spectrum of neurological and behavioral defects, clinically known as manganism. Therefore, manganese balance in the body needs to be tightly controlled to prevent its inadequacy or overload. Two organs, namely the intestine and the liver, play important roles in this control [1–4]. The intestine serves as the site for dietary manganese absorption [5–7]. After being absorbed into the blood circulation, manganese travels through the portal vein and is delivered to the liver where it can be stored, redistributed, or secreted as a bile conjugate for intestinal reabsorption or fecal excretion [1,8–13]. Manganese transporters expressed in the intestine and the liver are central to the regulation of systemic manganese metabolism.

ZIP14 (also known as solute carrier family 39 member 14, or *SLC39A14*) is a newly identified manganese transporter [14–16]. A genome-wide transcriptomics analysis of tissue samples from healthy individuals revealed that the greatest ZIP14 abundance is in the liver, followed by the small intestine—the two main organs involved in regulating systemic manganese metabolism [17]. Indeed, patients carrying loss-of-function mutations of *ZIP14* developed manganese toxicity and early-onset dystonia due to manganese hyperaccumulation in the brain [18–22]. Consistent with the human phenotype associated with *ZIP14* deficiency, mice with whole-body *Zip14* knockout (*Zip14*^{−/−}) exhibited manganese loading in the blood and the brain that were over 10 times the normal level [23–25], further indicating the indispensable role of ZIP14 in maintaining systemic manganese homeostasis.

Based on the observations that patients with a ZIP14 deficiency lacked hepatic manganese deposition and that *Zip14*^{−/−} mice had reduced liver manganese, it was initially

proposed that the inactivation of ZIP14 primarily impaired manganese delivery to the liver and subsequent clearance through biliary excretion, which in turn caused manganese accumulation in other organs including the brain [18]. However, liver-specific *Zip14*-knockout (*Zip14*-L-KO) mice did not display manganese hyperaccumulation in the blood or brain, despite significantly reduced liver manganese [25,26], in contrast with the results in *Zip14*^{-/-} mice.

In addition to the liver, the intestine also expresses high levels of ZIP14. Recent studies using intestine-specific *Zip14*-knockout (*Zip14*-In-KO) mice demonstrated a critical role for intestinal ZIP14 in controlling systemic manganese homeostasis because *Zip14*-In-KO mice developed increased manganese in both the blood and the brain [26,27]. However, the brain manganese loading observed in *Zip14*-In-KO mice was much less severe when compared with that seen in *Zip14*^{-/-} mice of a similar age [26,28]. We hypothesized that, since hepatic ZIP14 was intact in *Zip14*-In-KO mice, excess manganese resulting from increased manganese absorption could be partially removed through hepatobiliary excretion, leading to less severe manganese loading in *Zip14*-In-KO mice. Therefore, the present study aimed to further elucidate the mechanism of systemic manganese homeostatic regulation by examining manganese levels in mice with ZIP14 knockout in both the intestine and the liver (*Zip14* double knockout, or *Zip14*-DKO).

2. Materials and Methods

2.1. Animals, Genotyping and Tissue Collection

All procedures for animal experiments were approved by the Institutional Animal Care and Use Committees (IACUC) of the University of Arizona (Protocol number: 16–172). Animal cages containing less than 5 mice were kept at 21–22 °C with 12 h light/dark cycles. Mice were provided with tap water *ad libitum*, and fed a traditional rodent diet (Teklad 7913; Envigo, Indianapolis, IN, USA). Mice carrying the *Zip14* conditional allele (*Zip14*^{flox/flox}) have been described previously [26]. Mice expressing Cre recombinase under the intestine-specific (Vil-Cre) or liver-specific (Alb-Cre) promoter were purchased from the Jackson Laboratory (Bar Harbor, ME, USA). *Zip14*^{flox/flox} mice were bred with Vil-Cre or Alb-Cre mice to obtain *Zip14*^{flox/-}Vil-Cre⁺ or *Zip14*^{flox/-}Alb-Cre⁺ mice. *Zip14*^{flox/-}Vil-Cre⁺ and *Zip14*^{flox/-}Alb-Cre⁺ mice were then crossbred to produce *Zip14*^{flox/-}Vil-Cre⁺Alb-Cre⁺ mice. To generate tissue-specific *Zip14* knockout and the control littermates, *Zip14*^{flox/-}Vil-Cre⁺Alb-Cre⁺ mice were bred to produce all four mouse strains used in this study, including *Zip14*^{flox/flox} (control), *Zip14*^{flox/flox}Vil-Cre⁺ (*Zip14*-In-KO), *Zip14*^{flox/flox}Alb-Cre⁺ (*Zip14*-L-KO), and *Zip14*^{flox/flox}Vil-Cre⁺Alb-Cre⁺ (*Zip14*-DKO). A Mouse Direct PCR kit (Bimake, Houston, TX, USA) and the following primers were used to determine animal genotypes. For *Zip14*^{flox/flox} mice: Forward, 5'-GAT TCC TCC AAA GTC AAG TAG AGC G-3'; Reverse, 5'-GCT TGG AAG GGC TGG GTG CA-3'. Genotyping procedures for Vil-Cre and Alb-Cre mice were performed according to the company's instructions. All mice were sacrificed at 9 weeks of age after anesthesia with ketamine/xylazine. Blood samples were collected via cardiac puncture. Mouse tissues were immediately frozen in liquid nitrogen after collection and stored in a -80 °C freezer for further analyses.

2.2. Metal Content Measurement

The metal contents of mouse tissues were analyzed by inductively coupled plasma mass spectrometry (ICP-MS) at the Arizona Laboratory for Emerging Contaminants (ALEC). Frozen tissues were weighed and dried in an oven at 80 °C for at least 2 days until they reached a constant weight. Dried tissues were digested with 2 mL of 70% concentrated HNO₃ at room temperature (RT) overnight, and then at 80 °C for 6 h, followed by 60 °C overnight. Tissue digests (400 µL) were diluted using 9 mL of Milli-Q water to a total volume of 9.4 mL at a final concentration of 3% HNO₃. For blood samples, 50 µL of blood was digested in 280 µL of 70% HNO₃, incubated overnight at RT, and then at 80 °C for 4 h. The digested samples (200 µL) were diluted in 3.8 mL of Milli-Q water to a total volume of 4 mL at a final concentration of 3% HNO₃. The metal contents were analyzed using the

Agilent 7700 × ICP-MS instrument (Agilent Technologies, Santa Clara, CA, USA) at the ALEC. The protocol for analytical QA/QC was adapted from US EPA Method 200.8 for ICP-MS analysis. A multi-element stock solution (SPEX CertiPrep, Metuchen, NJ, USA) was used to prepare calibration standards, including at least 7 points with correlation coefficients higher than 0.995. The QC protocol included a continuing calibration blank, a continuing calibration verification solution, and at least one quality control sample to be analyzed after calibration, after 12 samples and at the completion of all sample analyses. Acceptable QC responses were between 90% and 110% of the certified values.

2.3. Western Blot Analysis

Mouse tissues were lysed in NETT buffer (150 mM NaCl, 5 mM EDTA, 10 mM Tris, 1% Triton X-100, and 1× Protease inhibitor cocktail). Protein concentrations were determined using the RC DC protein assay (Bio-Rad Life Science, Hercules, CA, USA). Equal amounts of protein were mixed with Laemmli buffer and incubated at 37 °C for 30 min. Proteins were electrophoretically separated on 10% sodium dodecyl sulfate polyacrylamide gels and transferred to nitrocellulose membranes (GVS, Sanford, ME, USA). After 1 h incubation with blocking buffer (5% non-fat dry milk in TBST (10 mM Tris/HCl, 150 mM NaCl, 0.1% 1 mL Tween-20, pH 7.5)) at RT, membranes were incubated with rabbit anti-mZIP14 antibody (1:1000) overnight at 4 °C. The generation of anti-mZIP14 antibody was described previously [26]. After incubation with the anti-mZIP14 antibody, nitrocellulose membranes were then washed 4 times with TBST (5 min/wash), and incubated for 1 h at RT with the donkey anti-rabbit horseradish peroxidase (HRP)-conjugated secondary antibody (1:5000) (GE healthcare, Chicago, IL, USA). Before imaging, membranes were washed two times (5 min/wash) with TBST, followed by two washes with TBS (5 min/wash) prior to imaging using the ChemiDoc MP system and Image Lab software (Bio-Rad). To confirm equivalent loading, the membranes were stripped for 15 min in Restore PLUS Western blotting stripping buffer (Thermo Fisher Scientific, Waltham, MA, USA), blocked for 1 h in blocking buffer, and reprobbed with HRP-conjugated antibodies against GAPDH (1:20,000) or beta-ACTIN (1:20,000, Proteintech, Rosemont, IL, USA).

2.4. Statistical Analysis

Data were expressed as mean ± standard deviation of the mean (SD). Data homogeneity of variance was determined using the Brown–Forsythe test for each dataset, and no significant differences in the SDs were found. Comparisons between groups in each dataset were performed by one-way analysis of variance (ANOVA) followed by Bonferroni’s post-hoc tests using PRISM 8 software (GraphPad, La Jolla, CA, USA). For the post-hoc comparisons, a *p*-value < 0.05 was considered statistically significant with: * *p* < 0.05; ** *p* < 0.01; *** *p* < 0.001 and **** *p* < 0.0001.

3. Results

3.1. Generation of Mice with Tissue-Specific *Zip14* Deletion

To determine the coordinated regulation of manganese metabolism by the intestine and the liver, we generated a double-tissue *Zip14*-knockout mouse model (*Zip14*-DKO) with the inactivation of *Zip14* in both the intestine and the liver, then collected animal tissues at 9 weeks of age. For comparison with the age-matched single-tissue *Zip14* knockout, we also generated mice with a *Zip14* deletion in the intestine or the liver (*Zip14*-In-KO or *Zip14*-L-KO mice). Western blot analyses of the liver (Figure 1A,B) and the intestine tissue samples (Figure 1C,D) confirmed that the ZIP14 protein was indeed absent in the corresponding sites of relevant single- or double-tissue-specific knockout mice.

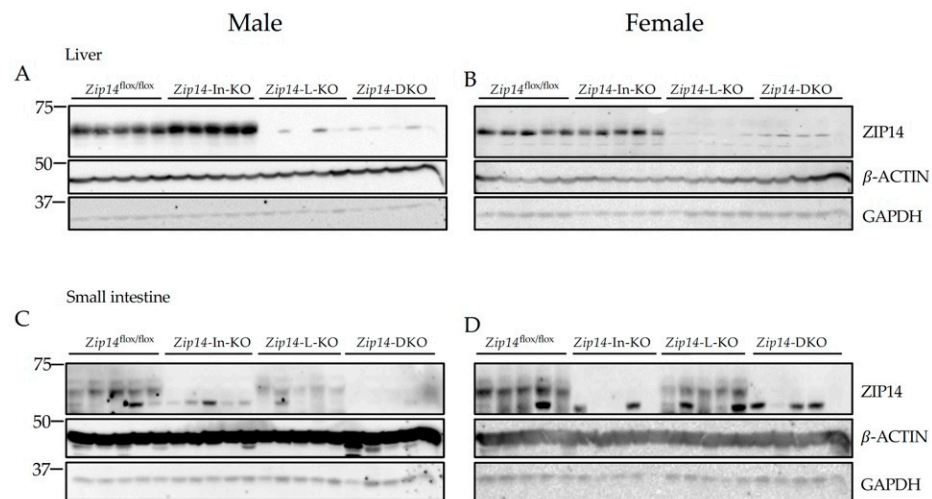


Figure 1. Western blot analyses to confirm tissue-specific *Zip14* knockout in mice. *Zip14*^{fllox/fllox} mice were bred with tissue-specific Cre transgenic mice to generate mice with *Zip14* knockout in the intestine, the liver, or in both tissues. Mice were sacrificed and tissues were collected at 9 weeks of age. Western blot images of (A,B) the liver and (C,D) small intestine samples from control (*Zip14*^{fllox/fllox}), intestine-specific *Zip14* KO (*Zip14*-In-KO), liver-specific *Zip14* KO (*Zip14*-L-KO), and (intestine and liver)-specific *Zip14* KO (*Zip14*-DKO) mice (A,C: male mice; B,D: female mice, *n* = 5). Both β -ACTIN and GAPDH were used as loading controls.

Reduced body weight was found to be a common phenotype of gene knockout in mice [29]. A previous report has found that with whole-body *Zip14* knockout, *Zip14*^{-/-} mice developed growth retardation, shorter body length, and lower body weight [30]. Therefore, we measured mouse body weights to determine the effect of tissue-specific *Zip14* deletion on animal growth. We found that body weight did not differ between the four animal genotypes examined in this study, (Figure 2A,B), indicating that mice grew at a similar rate between these groups.

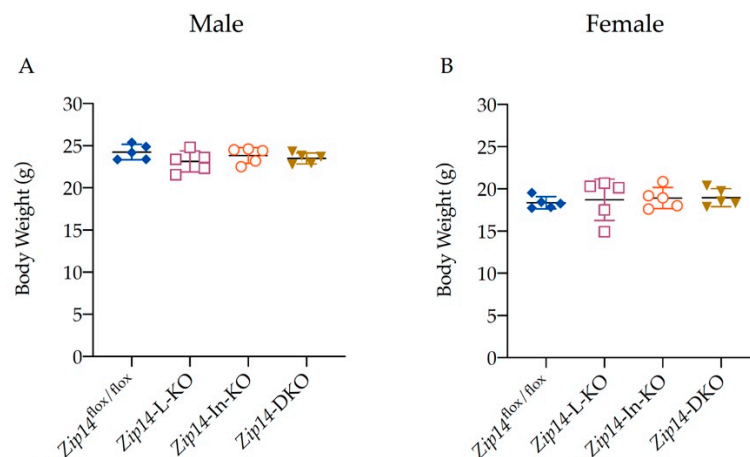


Figure 2. Deletion of ZIP14 in the intestine and/or liver did not affect the body weight in mice. Body weights of the 9-week-old control, *Zip14*-In-KO, *Zip14*-L-KO, and *Zip14*-DKO mice were plotted. (A) Male mice (*n* = 5). (B) Female mice (*n* = 5). Data were expressed as mean \pm standard deviation (SD). Statistical analysis was performed using one-way analysis of variance (ANOVA) followed by the Bonferroni post-hoc test. No significant differences were found between these groups.

3.2. Blood Manganese Increases Significantly in *Zip14*-DKO Mice

Since whole-blood manganese content can be used as an indicator for body manganese status in rodents [31], we first measured manganese content in the blood using ICP-MS analysis. Consistent with previous reports [25,26], we found that there was no significant

difference in blood manganese between the 9-week-old control and *Zip14*-L-KO mice, suggesting that the hepatic ZIP14 does not serve as a primary regulator for systemic manganese homeostasis under normal conditions (Figure 3A,B). In contrast, the blood manganese in the 9-week-old *Zip14*-In-KO mice was about 2.4 times and 1.4 times as high as the control values for male and female mice, respectively ($0.0402 \pm 0.0047 \mu\text{g}/\text{mL}$ vs. $0.0965 \pm 0.0480 \mu\text{g}/\text{mL}$ for male mice; $0.0477 \pm 0.0042 \mu\text{g}/\text{mL}$ vs. $0.0671 \pm 0.0087 \mu\text{g}/\text{mL}$ for female mice), indicating that the deletion of intestinal ZIP14 increased the body's manganese burden (Figure 3A,B).

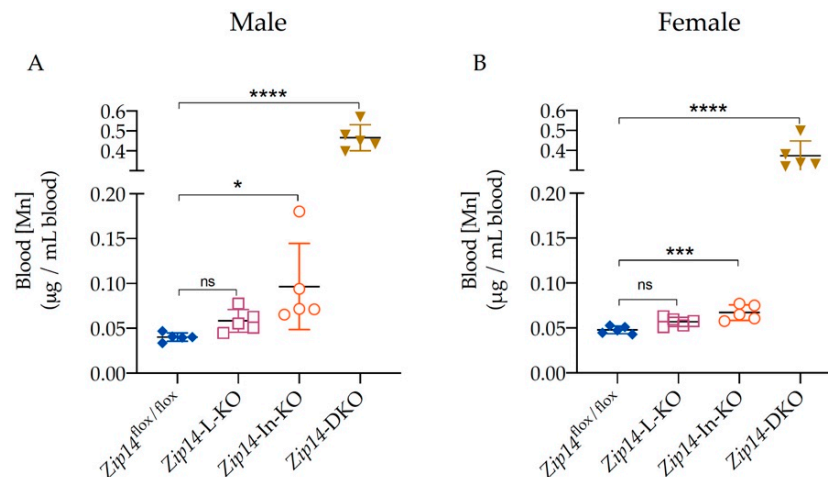


Figure 3. Blood manganese increased significantly in *Zip14*-DKO mice. Blood manganese (Mn) concentrations were measured by inductively coupled plasma mass spectrometry (ICP-MS) for (A) male mice ($n = 5$) and (B) female mice ($n = 5$) at 9 weeks of age. Data were expressed as mean \pm SD and were subjected to a one-way ANOVA followed by the Bonferroni post-hoc test to compare the mean of each knockout group to the control group. * $p < 0.05$, *** $p < 0.001$ and **** $p < 0.0001$. “ns” indicates no significant differences.

However, the extent of manganese accumulation caused by the loss of intestinal ZIP14 was not as severe as that observed in *Zip14*^{-/-} mice because it has been reported that the blood manganese levels in *Zip14*^{-/-} mice of a similar age were about 15 times as high as the wild-type (WT) littermates [28]. We hypothesize that since hepatic ZIP14 was intact in *Zip14*-In-KO mice, excess manganese resulting from the loss of intestinal ZIP14 could be partially removed through hepatobiliary excretion, leading to less severe manganese loading in *Zip14*-In-KO mice. Indeed, with the deletion of both intestinal and hepatic ZIP14, *Zip14*-DKO mice had a blood manganese concentration about 12 times ($0.0402 \pm 0.0047 \mu\text{g}/\text{mL}$ vs. $0.4666 \pm 0.0652 \mu\text{g}/\text{mL}$ for male mice) or 8 times ($0.0477 \pm 0.0042 \mu\text{g}/\text{mL}$ vs. $0.3734 \pm 0.0740 \mu\text{g}/\text{mL}$ for female mice) as high as the value of sex-matched littermate controls (Figure 3A,B), indicating that both intestinal and hepatic ZIP14 contributed to the regulation of systemic manganese homeostasis.

As a divalent metal transporter, ZIP14 can mediate the transport of a variety of essential trace metals including zinc [14]. ICP-MS measurements demonstrated that, in contrast to the significantly altered blood manganese, blood zinc levels did not differ between the four groups of mice examined in this study (Figure 4A,B), suggesting that loss of ZIP14 in the intestine and/or in the liver did not significantly affect the body's zinc metabolism.

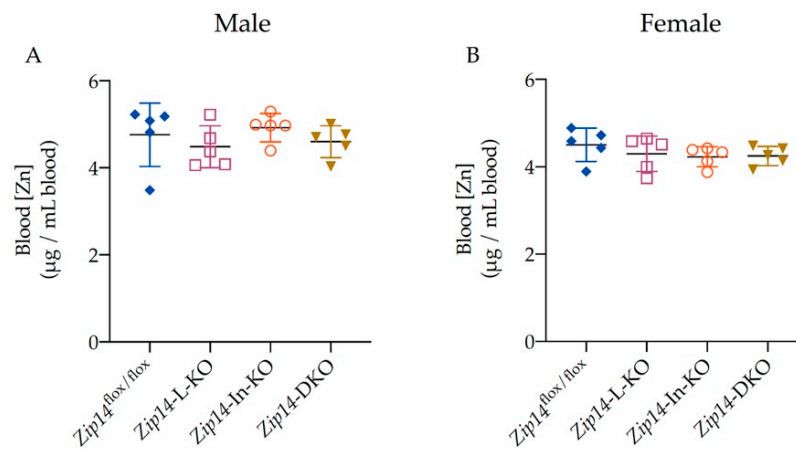


Figure 4. Tissue-specific *Zip14* knockout did not alter blood zinc levels. Blood zinc (Zn) concentrations were measured by ICP-MS for (A) male ($n = 5$) and (B) female mice ($n = 5$). Data were expressed as mean \pm SD and statistical analysis was performed using one-way ANOVA followed by the Bonferroni post-hoc test. No significant difference was observed between each group of *Zip14* knockout and control mice.

3.3. Liver Manganese Increases in *Zip14-In-KO* Mice, but Decreases Significantly in Both *Zip14-L-KO* and *Zip14-DKO* Mice

To further determine the effect of tissue-specific *Zip14* knockout, we next analyzed liver manganese. The 9-week-old *Zip14-L-KO* mice had about 90–95% decreased manganese content in the liver when compared with the sex-matched *Zip14^{flox/flox}* control animals (Figure 5A,B) ($5.648 \pm 1.18 \mu\text{g/g}$ vs. $0.3069 \pm 0.1494 \mu\text{g/g}$ for male mice; $5.843 \pm 0.8622 \mu\text{g/g}$ vs. $0.6499 \pm 0.2523 \mu\text{g/g}$ for female mice). These results support the notion that ZIP14 is the major transporter mediating manganese uptake into the liver [24–26]. In contrast, for *Zip14-In-KO* mice, a significant increase in liver manganese (increased by 28% in male mice and by 38% in female mice) was evident (Figure 5A,B), reinforcing the idea that the deletion of intestinal ZIP14 increases the body's manganese burden. Similar to *Zip14-L-KO* mice, *Zip14-DKO* mice displayed reduced liver manganese when compared with *Zip14^{flox/flox}* control mice, indicating that the hepatic manganese accumulation was impaired in both *Zip14-L-KO* and *Zip14-DKO* mice.

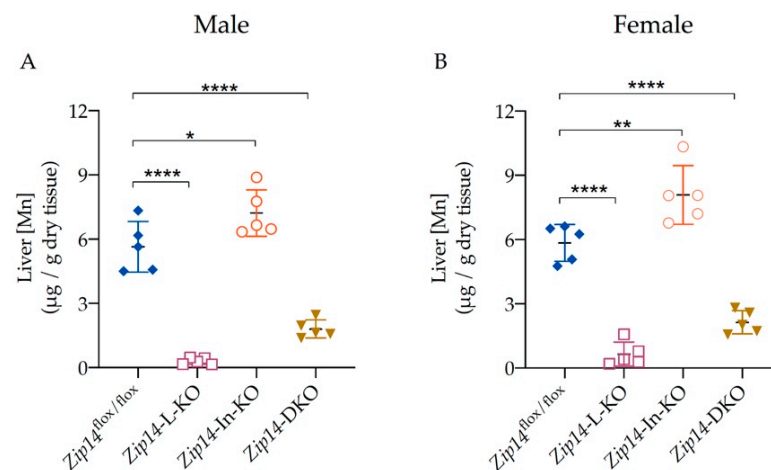


Figure 5. Liver manganese increased in *Zip14-In-KO* mice but decreased in both *Zip14-L-KO* and *Zip14-DKO* mice. Liver Mn contents were measured by ICP-MS in (A) male ($n = 5$) and (B) female mice ($n = 5$). Data were expressed as mean \pm SD and were subjected to a one-way ANOVA followed by the Bonferroni post-hoc test to compare the mean of each knockout group to the control group. * $p < 0.05$, ** $p < 0.01$ and **** $p < 0.0001$.

3.4. ZIP14 Deletion in Both the Liver and Intestine Significantly Increases Brain Manganese Accumulation

ZIP14 inactivation primarily impairs the central nervous system and leads to neurodegenerative symptoms due to manganese hyperaccumulation in the brain. For example, the brain manganese in 6-to-12-week-old *Zip14*^{-/-} mice was reported to be about 10 times as high as that in WT mice [28]. In the present study, we examined the effect of tissue-specific *Zip14* deletion on brain manganese in 9-week-old mice and found that *Zip14*-L-KO mice had normal brain manganese while *Zip14*-In-KO mice developed increased brain manganese loading (increased by 40% in male mice and by 20% in female mice) when compared with the *Zip14*^{fllox/fllox} control mice (Figure 6A,B). These results further demonstrated an increased systemic manganese burden with the loss of intestinal ZIP14. Importantly, with the deletion of ZIP14 in both the intestine and the liver, *Zip14*-DKO mice displayed exacerbated manganese loading in the brain (5.5 times and 4.6 times as high as the controls for male and female mice, respectively), demonstrating that the liver works in tandem with the intestine to regulate systemic manganese homeostasis.

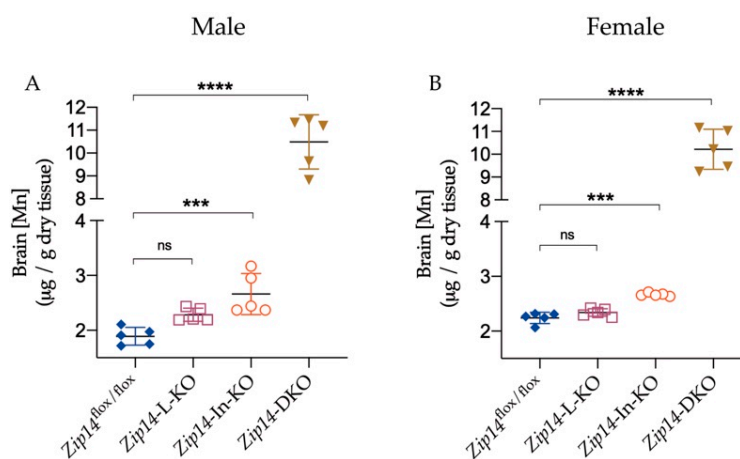


Figure 6. Combined inactivation of intestinal and hepatic ZIP14 greatly exacerbated brain manganese accumulation. Brain Mn concentrations were measured by ICP-MS in (A) male ($n = 5$) or (B) female mice ($n = 5$). Data were expressed as mean \pm SD and were subjected to a one-way ANOVA followed by the Bonferroni post-hoc test to compare the mean of each knockout group to the control group. *** $p < 0.001$ and **** $p < 0.0001$. “ns” indicates no significant differences.

4. Discussion

Manganese metabolism needs to be tightly regulated to prevent adverse effects caused by an excess or a deficiency of this trace nutrient. Intestinal absorption and hepatobiliary excretion of manganese are two important physiological processes for the regulation of systemic manganese homeostasis [32–35]. However, mechanisms underlying such regulation are not well understood. ZIP14 is a newly identified manganese importer with high expression levels in both the small intestine and the liver. Patients with loss-of-function mutations in *ZIP14* developed severe childhood-onset neurological disorders due to manganese accumulation in the brain; similarly, mice with whole-body *Zip14* knockout displayed manganese loading in the blood and brain at over 10 times the normal level, indicating an indispensable role for ZIP14 in maintaining systemic manganese homeostasis [18,19,21–25].

When the initial cases of *ZIP14* mutations in patients or *Zip14* knockout in mice were reported, it was thought that manganese hyperaccumulation caused by ZIP14 loss was primarily due to impaired manganese delivery to the liver, which in turn decreased manganese excretion through the bile, and caused manganese accumulation in the blood and other tissues, such as the brain. However, with hepatic ZIP14 inactivation, *Zip14*-L-KO mice had reduced liver manganese without developing manganese overload in other organs, indicating that hepatic ZIP14 was not the primary control for systemic manganese homeostasis under normal physiological conditions [25,26]. Then, a question arose naturally:

How does hepatic ZIP14 contribute to the maintenance of systemic manganese homeostasis? In contrast to the results obtained from *Zip14*-L-KO mice, with intestinal ZIP14 inactivation, *Zip14*-In-KO mice displayed an increased manganese loading in both the liver and the brain, demonstrating an essential role for intestinal ZIP14 in regulating whole-body manganese metabolism [26,27]. However, the extent of brain manganese loading observed in *Zip14*-In-KO mice was rather mild when compared with that in *Zip14*^{-/-} mice. These results opened up a new question: Could the relatively mild degree of manganese loading in *Zip14*-In-KO mice be ascribed to the presence of hepatic ZIP14, which may facilitate the removal of excess manganese through the route of hepatobiliary excretion?

The present study created *Zip14*-DKO mice with *Zip14* inactivation in both the intestine and the liver to further reveal the mechanisms underlying ZIP14's function in manganese metabolism. Age- and sex-matched *Zip14*-L-KO and *Zip14*-In-KO mice were also analyzed for comparison. Our results clearly showed that the deletion of both intestinal and hepatic ZIP14 exacerbated manganese loading in mice when compared with either single-tissue knockout (Figures 3, 5 and 6). Our findings indicate that, while the intestinal ZIP14 serves as a primary control for manganese metabolism, the hepatic ZIP14 is also essential for the maintenance of systemic manganese homeostasis under normal physiological conditions. The intestine and the liver are central for the regulation of nutrient metabolism. Our study demonstrated that combined defects in these two organs account for the onset of dysregulated manganese homeostasis seen in individuals lacking ZIP14.

In summary, the present study demonstrated, for the first time, the coordinated regulation of systemic manganese homeostasis by both intestinal and hepatic ZIP14, and enhanced our understanding of the disease mechanism underlying systemic manganese overload associated with ZIP14 loss.

Author Contributions: Conceptualization, N.Z.; Methodology, C.K.F. and N.Z.; Validation, C.K.F. and N.Z.; Formal Analysis, C.K.F. and N.Z.; Investigation, C.K.F. and N.Z.; Resources, N.Z.; Writing—Original Draft Preparation, C.K.F. and N.Z.; Writing—Review and Editing, C.K.F. and N.Z.; Supervision, N.Z.; Project Administration, N.Z.; Funding Acquisition, N.Z. All authors have read and agreed to the published version of the manuscript.

Funding: Research reported in this publication was supported by the National Institute of Diabetes and Digestive and Kidney Diseases (NIDDK) and the Office of Dietary Supplements (ODS) of the National Institutes of Health (NIH) (R01DK123113). The content is solely the responsibility of the authors and does not necessarily represent the official views of the National Institutes of Health.

Institutional Review Board Statement: Procedures for animal experiments were approved by the Institutional Animal Care and Use Committee of the University of Arizona.

Informed Consent Statement: Not applicable.

Data Availability Statement: The data presented in this study are available on request from the corresponding author.

Acknowledgments: We thank Shannon McCabe for the critical reading of this manuscript. We thank Mary Kay Amistadi in the Arizona Laboratory for Emerging Contaminants for the help with ICP-MS measurement.

Conflicts of Interest: The authors declare no conflict of interest.

References

1. Chen, P.; Bornhorst, J.; Aschner, M. Manganese metabolism in humans. *Front. Biosci.* **2018**, *23*, 1655–1679. [[CrossRef](#)] [[PubMed](#)]
2. Aschner, J.L.; Aschner, M. Nutritional aspects of manganese homeostasis. *Mol. Asp. Med.* **2005**, *26*, 353–362. [[CrossRef](#)] [[PubMed](#)]
3. O'Neal, S.L.; Zheng, W. Manganese Toxicity Upon Overexposure: A Decade in Review. *Curr. Environ. Health Rep.* **2015**, *2*, 315–328. [[CrossRef](#)] [[PubMed](#)]
4. Avila, D.S.; Puntel, R.L.; Aschner, M. Manganese in health and disease. *Met. Ions Life Sci.* **2013**, *13*, 199–227. [[CrossRef](#)]
5. Garcia-Aranda, J.A.; Wapnir, R.A.; Lifshitz, F. In vivo intestinal absorption of manganese in the rat. *J. Nutr.* **1983**, *113*, 2601–2607. [[CrossRef](#)]

6. Lutz, T.A.; Schroff, A.; Scharrer, E. Effects of calcium and sugars on intestinal manganese absorption. *Biol. Trace Elem. Res.* **1993**, *39*, 221–227. [[CrossRef](#)]
7. Miller, W.J. Dynamics of absorption rates, endogenous excretion, tissue turnover, and homeostatic control mechanisms of zinc, cadmium, manganese, and nickel in ruminants. *Fed. Proc.* **1973**, *32*, 1915–1920.
8. Roth, J.A. Homeostatic and toxic mechanisms regulating manganese uptake, retention, and elimination. *Biol. Res.* **2006**, *39*, 45–57. [[CrossRef](#)]
9. Schroeder, H.A.; Balassa, J.J.; Tipton, I.H. Essential trace metals in man: Manganese. A study in homeostasis. *J. Chronic Dis.* **1966**, *19*, 545–571. [[CrossRef](#)]
10. Butterworth, R.F. Parkinsonism in cirrhosis: Pathogenesis and current therapeutic options. *Metab. Brain Dis.* **2013**, *28*, 261–267. [[CrossRef](#)]
11. Burnett, W.T., Jr.; Bigelow, R.R.; Kimball, A.W.; Sheppard, C.W. Radio-manganese studies on the mouse, rat and pancreatic fistula dog. *Am. J. Physiol.* **1952**, *168*, 620–625. [[CrossRef](#)] [[PubMed](#)]
12. Cotzias, G.C.; Papavasiliou, P.S. Primordial Homeostasis in a Mammal as Shown by the Control of Manganese. *Nature* **1964**, *201*, 828–829. [[CrossRef](#)]
13. Bertinchamps, A.J.; Miller, S.T.; Cotzias, G.C. Interdependence of routes excreting manganese. *Am. J. Physiol.* **1966**, *211*, 217–224. [[CrossRef](#)] [[PubMed](#)]
14. Pinilla-Tenas, J.J.; Sparkman, B.K.; Shawki, A.; Illing, A.C.; Mitchell, C.J.; Zhao, N.; Liuzzi, J.P.; Cousins, R.J.; Knutson, M.D.; Mackenzie, B. Zip14 is a complex broad-scope metal-ion transporter whose functional properties support roles in the cellular uptake of zinc and nontransferrin-bound iron. *Am. J. Physiol. Cell Physiol.* **2011**, *301*, C862–C871. [[CrossRef](#)]
15. Girijashanker, K.; He, L.; Soleimani, M.; Reed, J.M.; Li, H.; Liu, Z.; Wang, B.; Dalton, T.P.; Nebert, D.W. Slc39a14 gene encodes ZIP14, a metal/bicarbonate symporter: Similarities to the ZIP8 transporter. *Mol. Pharmacol.* **2008**, *73*, 1413–1423. [[CrossRef](#)] [[PubMed](#)]
16. Fujishiro, H.; Yano, Y.; Takada, Y.; Tanihara, M.; Himeno, S. Roles of ZIP8, ZIP14, and DMT1 in transport of cadmium and manganese in mouse kidney proximal tubule cells. *Metallomics* **2012**, *4*, 700–708. [[CrossRef](#)] [[PubMed](#)]
17. Fagerberg, L.; Hallstrom, B.M.; Oksvold, P.; Kampf, C.; Djureinovic, D.; Odeberg, J.; Habuka, M.; Tahmasebpour, S.; Danielsson, A.; Edlund, K.; et al. Analysis of the human tissue-specific expression by genome-wide integration of transcriptomics and antibody-based proteomics. *Mol. Cell. Proteom.* **2014**, *13*, 397–406. [[CrossRef](#)]
18. Tuschl, K.; Meyer, E.; Valdivia, L.E.; Zhao, N.; Dadswell, C.; Abdul-Sada, A.; Hung, C.Y.; Simpson, M.A.; Chong, W.K.; Jacques, T.S.; et al. Mutations in SLC39A14 disrupt manganese homeostasis and cause childhood-onset parkinsonism-dystonia. *Nat. Commun.* **2016**, *7*, 11601. [[CrossRef](#)]
19. Marti-Sanchez, L.; Ortigoza-Escobar, J.D.; Darling, A.; Villaronga, M.; Baide, H.; Molero-Luis, M.; Batllori, M.; Vanegas, M.I.; Muchart, J.; Aquino, L.; et al. Hypermanganesemia due to mutations in SLC39A14: Further insights into Mn deposition in the central nervous system. *Orphanet J. Rare Dis.* **2018**, *13*, 28. [[CrossRef](#)]
20. Zeglam, A.; Abugrara, A.; Kabuka, M. Autosomal-recessive iron deficiency anemia, dystonia and hypermanganesemia caused by new variant mutation of the manganese transporter gene SLC39A14. *Acta Neurol. Belg.* **2019**, *119*, 379–384. [[CrossRef](#)]
21. Rodan, L.H.; Hauptman, M.; D’Gama, A.M.; Qualls, A.E.; Cao, S.; Tuschl, K.; Al-Jasmi, F.; Hertecant, J.; Hayflick, S.J.; Wessling-Resnick, M.; et al. Novel founder intronic variant in SLC39A14 in two families causing Manganism and potential treatment strategies. *Mol. Genet. Metab.* **2018**, *124*, 161–167. [[CrossRef](#)] [[PubMed](#)]
22. Juneja, M.; Shamim, U.; Joshi, A.; Mathur, A.; Uppili, B.; Sairam, S.; Ambawat, S.; Dixit, R.; Faruq, M. A novel mutation in SLC39A14 causing hypermanganesemia associated with infantile onset dystonia. *J. Gene Med.* **2018**, *20*, e3012. [[CrossRef](#)] [[PubMed](#)]
23. Aydemir, T.B.; Kim, M.H.; Kim, J.; Colon-Perez, L.M.; Banan, G.; Mareci, T.H.; Febo, M.; Cousins, R.J. Metal Transporter Zip14 (Slc39a14) Deletion in Mice Increases Manganese Deposition and Produces Neurotoxic Signatures and Diminished Motor Activity. *J. Neurosci.* **2017**, *37*, 5996–6006. [[CrossRef](#)]
24. Jenkitkasemwong, S.; Akinyode, A.; Paulus, E.; Weiskirchen, R.; Hojyo, S.; Fukada, T.; Giraldo, G.; Schrier, J.; Garcia, A.; Janus, C.; et al. SLC39A14 deficiency alters manganese homeostasis and excretion resulting in brain manganese accumulation and motor deficits in mice. *Proc. Natl. Acad. Sci. USA* **2018**, *115*, E1769–E1778. [[CrossRef](#)] [[PubMed](#)]
25. Xin, Y.; Gao, H.; Wang, J.; Qiang, Y.; Imam, M.U.; Li, Y.; Wang, J.; Zhang, R.; Zhang, H.; Yu, Y.; et al. Manganese transporter Slc39a14 deficiency revealed its key role in maintaining manganese homeostasis in mice. *Cell. Discov.* **2017**, *3*, 17025. [[CrossRef](#)] [[PubMed](#)]
26. Scheiber, I.F.; Wu, Y.; Morgan, S.E.; Zhao, N. The intestinal metal transporter ZIP14 maintains systemic manganese homeostasis. *J. Biol. Chem.* **2019**, *294*, 9147–9160. [[CrossRef](#)]
27. Aydemir, T.B.; Thorn, T.L.; Ruggiero, C.H.; Pompilus, M.; Febo, M.; Cousins, R.J. Intestine-specific deletion of metal transporter Zip14 (Slc39a14) causes brain manganese overload and locomotor defects of manganism. *Am. J. Physiol. Gastrointest. Liver Physiol.* **2020**, *318*, G673–G681. [[CrossRef](#)]
28. Wu, Y.; Wei, G.; Zhao, N. Restriction of Manganese Intake Prevents the Onset of Brain Manganese Overload in Zip14(-/-) Mice. *Int. J. Mol. Sci.* **2021**, *22*, 6773. [[CrossRef](#)]
29. Reed, D.R.; Lawler, M.P.; Tordoff, M.G. Reduced body weight is a common effect of gene knockout in mice. *BMC Genet.* **2008**, *9*, 4. [[CrossRef](#)]

30. Hojyo, S.; Fukada, T.; Shimoda, S.; Ohashi, W.; Bin, B.H.; Koseki, H.; Hirano, T. The zinc transporter SLC39A14/ZIP14 controls G-protein coupled receptor-mediated signaling required for systemic growth. *PLoS ONE* **2011**, *6*, e18059. [[CrossRef](#)]
31. Clegg, M.S.; Lonnerdal, B.; Hurley, L.S.; Keen, C.L. Analysis of whole blood manganese by flameless atomic absorption spectrophotometry and its use as an indicator of manganese status in animals. *Anal. Biochem.* **1986**, *157*, 12–18. [[CrossRef](#)]
32. Weigand, E.; Kirchgessner, M.; Helbig, U. True absorption and endogenous fecal excretion of manganese in relation to its dietary supply in growing rats. *Biol. Trace Elem. Res.* **1986**, *10*, 265–279. [[CrossRef](#)] [[PubMed](#)]
33. Britton, A.A.; Cotzias, G.C. Dependence of manganese turnover on intake. *Am. J. Physiol.* **1966**, *211*, 203–206. [[CrossRef](#)]
34. Dorman, D.C.; Struve, M.F.; James, R.A.; McManus, B.E.; Marshall, M.W.; Wong, B.A. Influence of dietary manganese on the pharmacokinetics of inhaled manganese sulfate in male CD rats. *Toxicol. Sci.* **2001**, *60*, 242–251. [[CrossRef](#)] [[PubMed](#)]
35. Davis, C.D.; Wolf, T.L.; Greger, J.L. Varying levels of manganese and iron affect absorption and gut endogenous losses of manganese by rats. *J. Nutr.* **1992**, *122*, 1300–1308. [[CrossRef](#)] [[PubMed](#)]